SUPPLEMENTAL INFORMATION

SUPPLEMENTAL EXPERIMENTAL PROCEDURES

Immunohistochemistry For mouse experiments, histology and immunohistochemistry were performed on paraffin-embedded or frozen sections from xenograft tumors as previously described (28). Intestinal, extra-GI tumor and corresponding normal tissues were snap frozen in OCT (Fisher Scientific, Pittsburgh, PA) and fixed in 10 % buffered formalin followed by paraffin embedding. For immunofluorescence, sections were immunostained with antibodies, counterstained with 4,6-diamidino-2-phenylindole (DAPI). H+E adjacent sections were used for comparison.

Immunocytochemistry. Cells were fixed with mixture of acetone and methanol (1:1) at -20℃ for 20 min, then rinsed three times with PBS. Following cells were incubated in a blocking solution (5% BSA or normal serum (goat, rabbit or horse) and 0.1% Triton-X in PBS) for 1 hour. For single or co-immunofluorescence staining, primary antibodies diluted in blocking solution were added overnight at 4℃ overnight. To ensure specificity, a no primary antibody control staining was performed. The slides were then washed in PBS and incubated with the appropriate secondary antibody for 1 hour at room temperature and counterstained/mounted with Vectashield containing DAPI (Vector Laboratories). Images were acquired on an inverted fluorescence microscope (Nikon Eclipse E800, Morrell Instruments). Ariol SL-50imaging software (Applied Imaging Instruments) was used to quantify biomarker staining. At least n=100 cells from three independent staining experiments were analyzed. Data are presented as means ± SEM and the significance was tested with the Student t test.

Fluorescent activated cell sorting (FACS) analysis FACS with anti-epithelial specific antigen (ESA, BD Pharmingen #347197) antibody was used to purify primary CRC cells (27, 67) or with anti-CCR9 antibody (BD Pharmingen Mountain View, CA) to sort CCR9+ and CCR9- CCIC, essentially as previously described (27, 67). Cells were first incubated with anti-human CCR9 antibody for 30 minutes on ice and then were washed in 1% BSA/PBS buffer. FACS was then used to separate CCIC into CCR9 positive and negative sub-groups by signal intensity gating. Approximately 6-8 hours after sorting, CCR9+ and CCR9- subsets from 1x 10^6 CCIC were inoculated into two mice by tail vein injection and monitored as described above. GFP-NOTCH FACS sorting was performed as described (44)**.**

Western Blotting

Isolated mouse intestine, lung tissues, cultured CCIC, or ATCC CRC cell lines were homogenized in RIPA buffer and complete protease inhibitor cocktail (Roche Applied Science, Indianapolis, IN)] with brief sonication on ice, and centrifuged for 5 minutes at 14,000 r.p.m to remove large debris. Protein concentration of the supernatant was determined by Bradford protein assay (Bio-Rad Laboratories Inc, Hercules, CA). Fifty micrograms of protein derived from tissue or cell lysates were separated by SDS-PAGE and transferred to polyvinylidenedifluoride membranes. Following blocking, membranes were probed with primary antibodies to determine different levels of protein expressions. Specific antibodies targeting CCR9 (Abcam, Cambridge, MA), CCL25 (R&D systems Inc; Minneapolis, MA, Cat# AF-481-NA), AKT (Cell Signaling, Inc, Cat# 9272), phospho-AKT (ser 473, Cell Signaling, Inc, Cat# 9271), phospho-AKT (thr 308, Cell Signaling, Inc,

Cat# 9275), GSK-3β (Cell Signaling, Inc, Cat# 9315), phosphor-GSK-3β (Cell Signaling, Inc, Cat# 9336), NICD (R&D Systems, Cat# AF3647), *HES1* (Santa Cruz, Cat# sc-13842), Snail (Cell Signaling, Cat# 3879), CD26 (Calbiochem, Cat# IM1004) were used, and anti-actin antibody (Santa Cruz Biotechnology Inc, Santa Cruz, CA, Cat# sc-1616-R) was used as internal controls. Immunoreactive antibody-antigen complexes were visualized with the enhanced chemiluminescence reagents from GE Healthcare (Uppsala, Sweden). The software of Quantity One (BioRad) was used to semi-quantify protein levels in western.

Generation of CCR9 constitutive expression CRC line.

The SureTiter TM lentivector (GenTarget Inc, San Diego, CA) in which the sub-cloned human CCR9 ORF sequence (gene ID: NM_006641) and a firefly luciferase gene were under control of CMV promoter was used to generate constitutively CCR9 expressing cell lines. To generate the lentiviral particles, the above plasmids were transfected into HEK293T cells with the Genetarget lentivirus packaging mix (GenTarget Inc, San Diego, CA) according to the manufacturer's protocol. The common used CRC line HCT116 was infected with lentivirus and positive cells selected by antibiotic.

Luciferase imaging in whole animal or ex vivo tissues:

Each NOG mouse was tail vein injected with 0.5x106 CCR9 constitutively expressing or scrambled control HCT116 cells and tumor formation was determined by luciferase-IVIS imaging system every 3 days For luciferase imaging, D-luciferin of 1.5mg/10g body weight was intra-peritoneally injected into mice and 10 min later, luciferase imaging (Xenogen IVIS-200) was applied on whole-mouse body or ex vivo tissues.

Cell proliferation assay

CCR9+ primary CRC and CCIC were FACS sorted and seeded in ultro-low attachment 24-well plates for 12 hours. 100ng/ml human CCL25, 1μg/ml CCR9 neutralizing antibody (R&D systems Inc;), 2 μM pan-AKT inhibitor Triciribine (Sigma) or control goat IgG were added into culture medium and cells were continued to incubate for 36 hours. The cellular ATP (adenosine triphosphate) levels were measured to quantify cell proliferation and viability using the ViaLightPlus Kit (Lonza Rockland, Inc.) and GloMax-20/20 Single-Tube Luminometer (Promega) per manufacture instructions.

SUPPLEMENTAL INFORMATION

All experiments were done with four to eight samples per group, and all results were derived from at least three independent experiments. Values are expressed as mean ± SEM. A *p* value less than 0.01 was considered significantly. Statistical calculations were performed with the Statistical Package for the Social Sciences version 11.5 software (SPSS Inc, Chicago, IL) or GraphPad. The statistical test used for each figure or table panel is indicated.

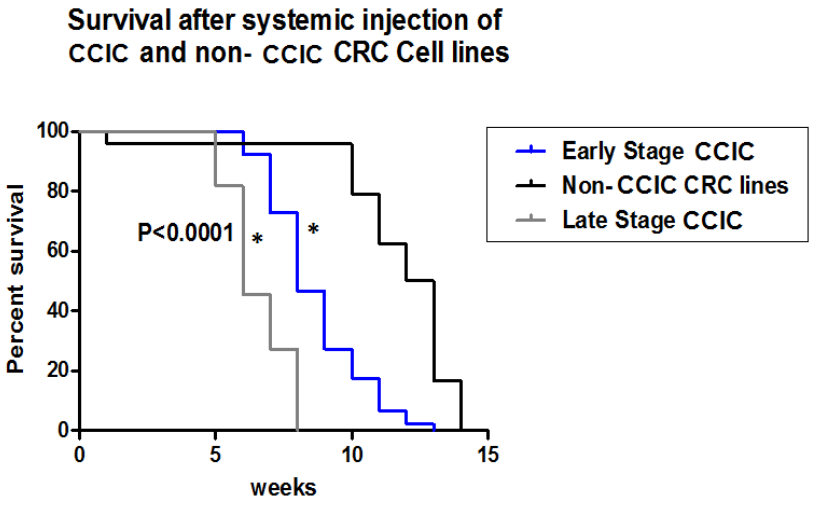

Supplemental Figure 1. Related to Figure 2. Survival of mice systemically injected with early stage CCICs, late stage CCICs and non-CCIC CRC lines. Kaplan-Meier survival analysis of mice after tail vein injection with early stage CCIC (blue), late stage CCIC (grey) or the non-CCIC commonly used CRC cell lines LoVo and SW480 (black). P<0.0001 difference between the early stage CCIC and commonly used CRC cell lines by log-rank test (Graphpad Prism software version 5).

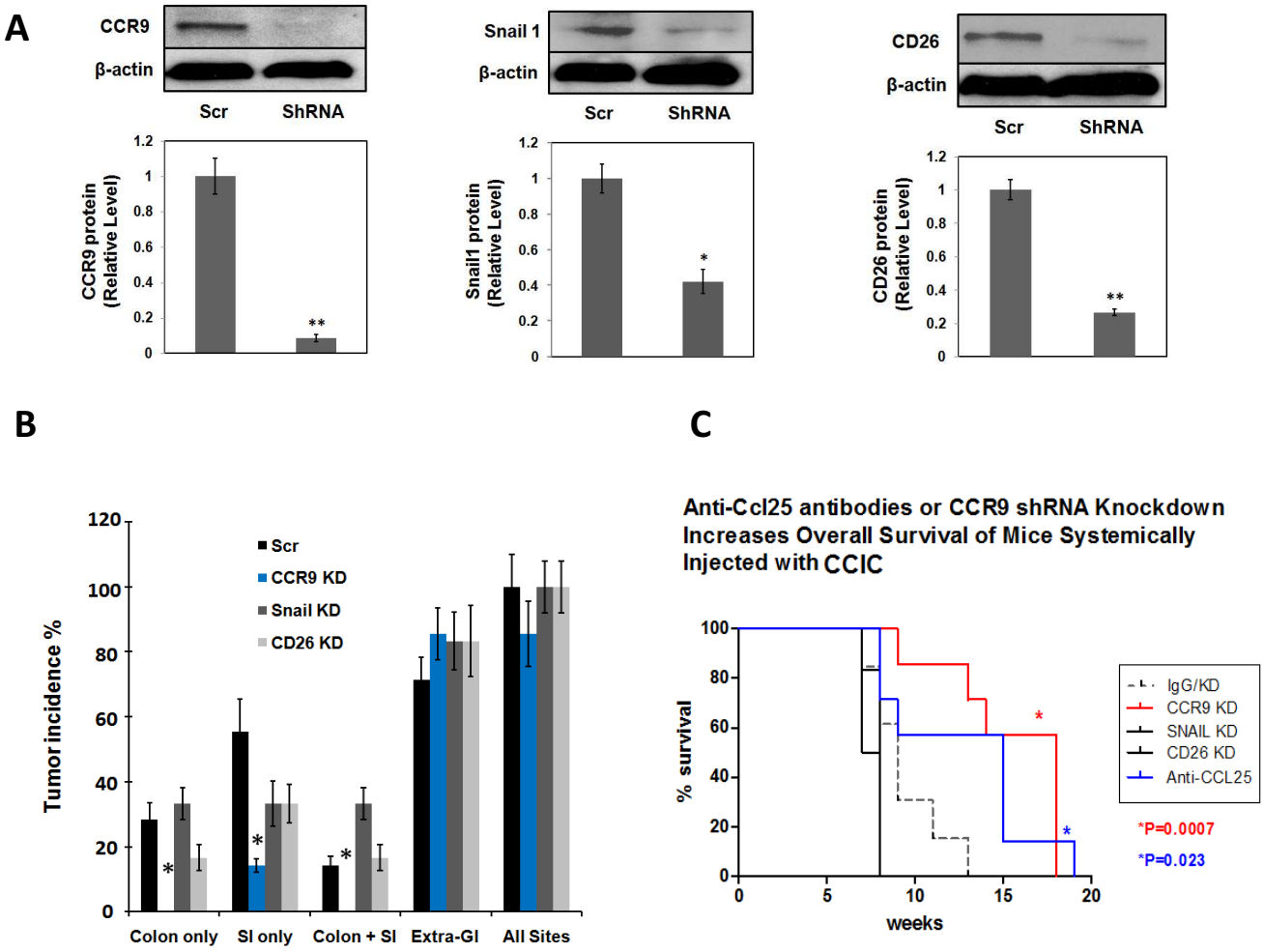

Supplemental Figure 2. Related to Figure 5. Anti-Ccl25 antibody systemic injection or shRNA knockdown of CCR9, but not CD26 or SNAIL, increases survival of mice systemically injected with CCIC. (A) shRNA constitutive knockdown efficiencies of CCR9, CD26 or SNAIL in CCIC were tested by western (left) and quantified (right) by using western quantification software of Quantitity One (BioRad). **(B)** Xenograft tumor incidence in mice injected with CCIC expressing anti-CCR9, SNAIL1 or CD26 shRNA knockdown, organized by tumor site. * P< 0.01 compared to scrambled shRNA control. Error bars indicate S.E.M**. (C)** Kaplan-Meier survival analysis of mice after tail vein injection with anti-Ccl25 antibodies or CCIC lentivirally infected with scrambled shRNA control (Mock), shRNA against CCR9, SNAIL1 or CD26. Survival curve data match Table 1. P=0.0007, Log Rank test comparison of overall survival of mice injected with CCIC expressing either scrambled shRNA control vector or anti-CCR9 knockdown sequences (Graphpad Prism version 5). P=0.023 Log Rank test comparison of overall survival of mice injected with anti-Ccl25 or IgG control (Graphpad Prism version 5).

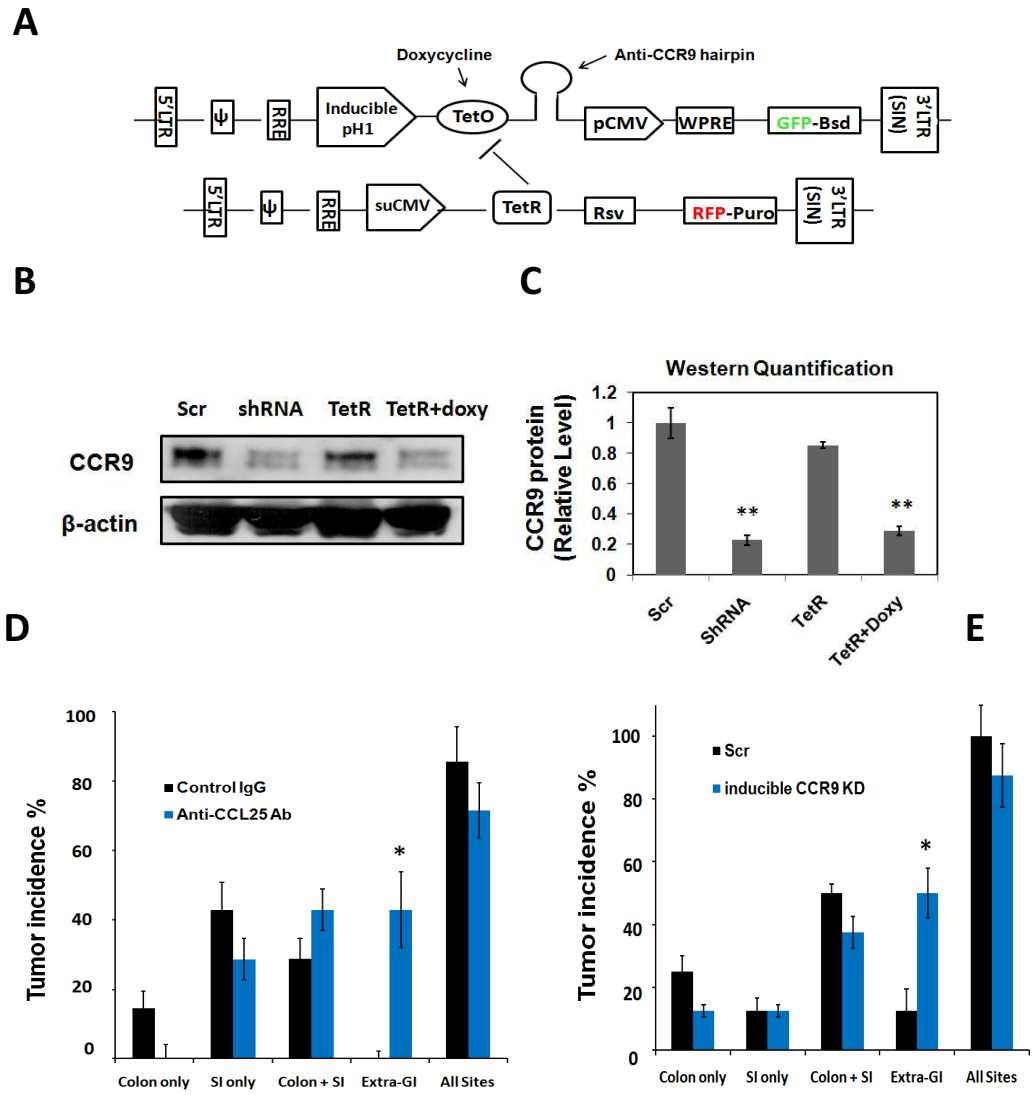

Supplemental Figure 3. related to Figure 6. CCR9/CCL25 signaling is inhibited after CCIC intestinal tumor initiation by anti-CCL25 antibody treatment or CCR9 inducible shRNA. **(A).** Schematic of CCR9 inducible shRNA, in which anti-CCR9 hairpin sequence was cloned in the 3'pH1 TetO promoter. Expression of anti-CCR9 hairpin was inhibited by TetR (Tet-repressor) and induced by tetrycycline derive doxycycline. **(B)**. Efficiency of CCR9 inducible knockdown in CCIC. The CCR9 protein levels in CCICs with only shRNAtetO vector, tetO + tetR or tetO+tetR+ doxycycline were detected by anti-human CCR9 antibody (left) and semi-quantified (right)by Quantitity One (BioRad).(**C & D**) Xenograft tumor incidence in mice injected with CCR9+ CCR9, and anti-CCL25 antibody therapy (**C**) or CCR9 inducible knockdown (or control, scr) by doxycycline (**D**) three weeks after tail vein injection organized by tumor site. * P< 0.01 compared to mock control. Error bars indicate S.E.M.

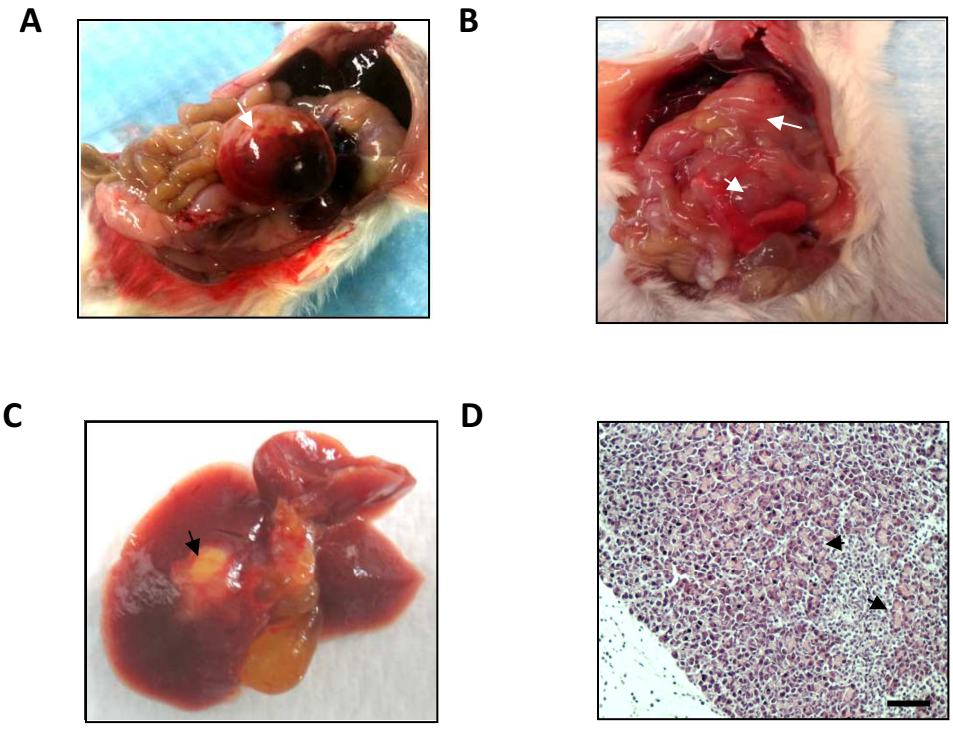

Supplemental Figure 4. related to Figure 6. CCIC extra-GI metastatic tumors are induced by anti-CCL25 treatment or CCR9 inducible knockdown. (A)and (B) Light microscopy of CCIC abdominal metastasis. **(C)** Light microscopy of CCIC liver metastasis, Metastatic foci are indicated by arrows. (**D**). H+E of CCIC metastatic tumors in pancreas. Arrows denote metastatic foci. Scale bar, 100μ.

A

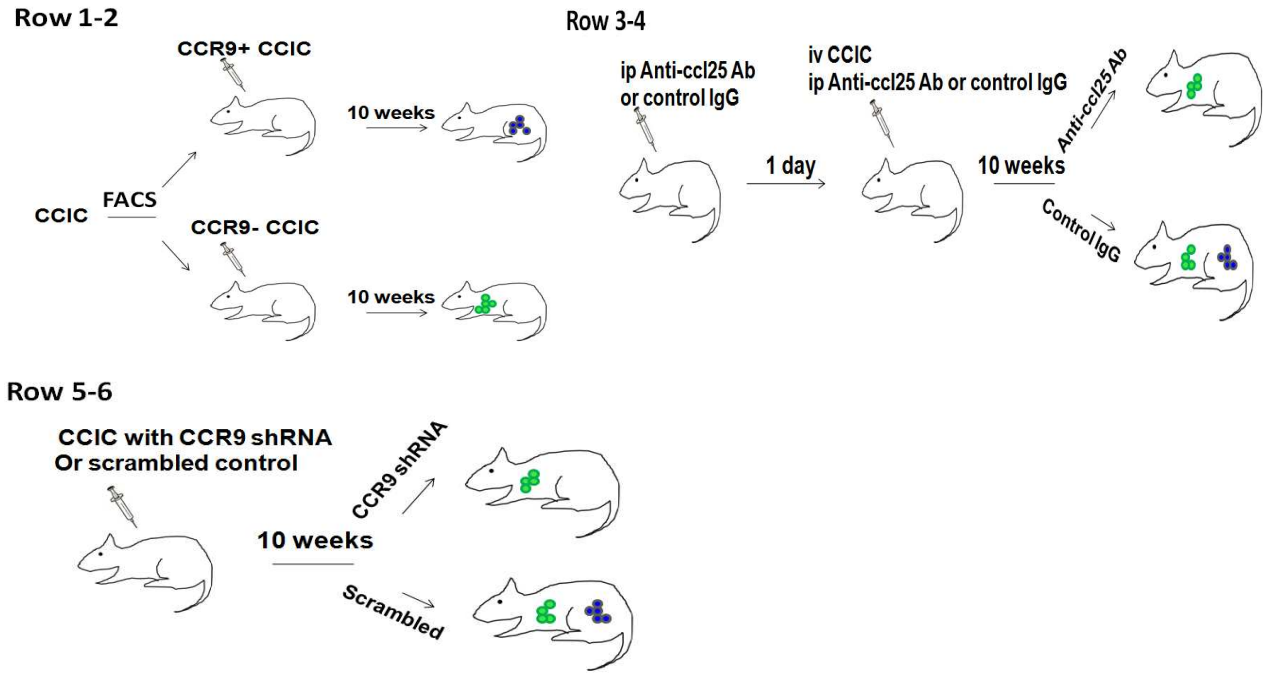

B

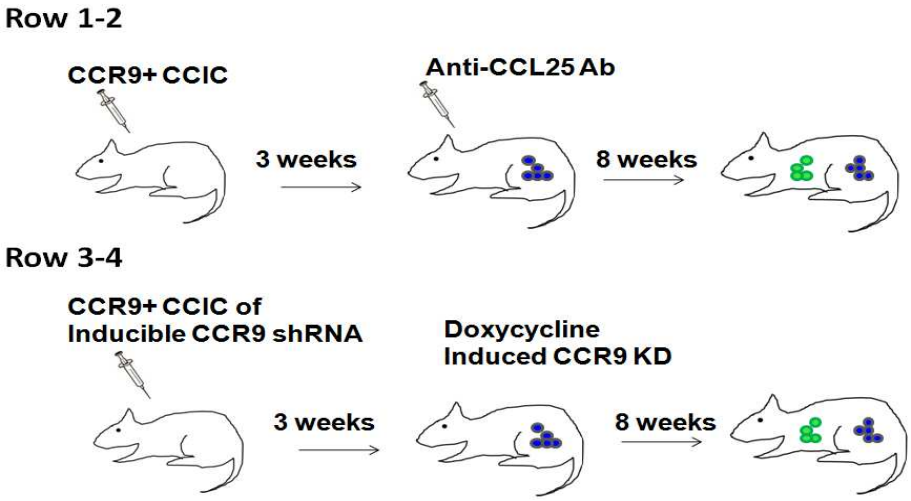

Supplemental Figure 5. related to Table 2 and 3. **(A).** Schema of the experimental procedures in Table 2. **(B)**Schema of the experimental procedures in Table 3. Colon/intestine tumors (blue) and ex-GI tumors (green) dots.

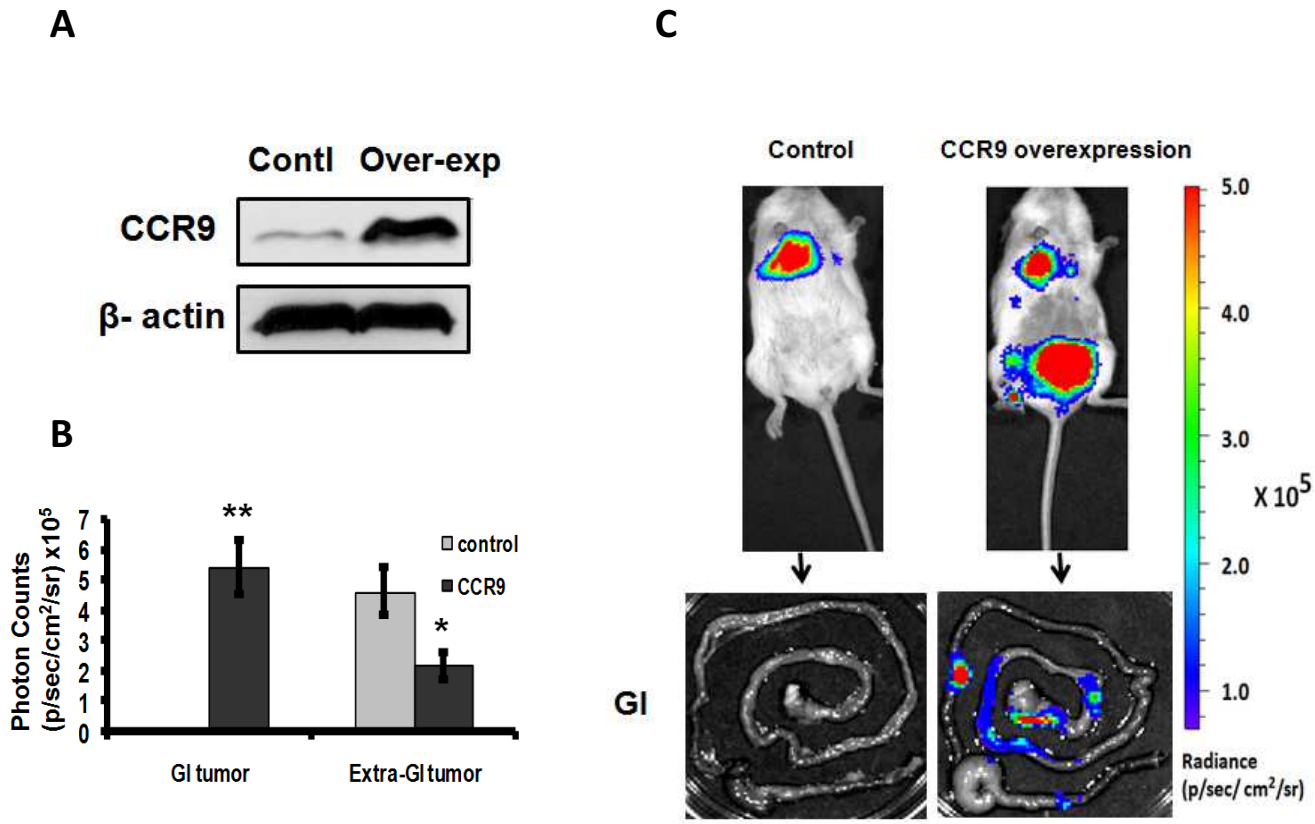

Supplemental Figure 6. Related to Figure 6. CCR9 overexpression in HCT116 significantly increased GI tumor formation and reduced extra-GI tumor formation (A). Western blot of CCR9 expression in HCT116 cells transfected with control vector or CCR9 constitutive expression vector. β-actin is loading control. (B). Quantification of GI and extra-GI tumors in mice that have HCT116 cells transfected with either CCR9 overexpression or control vector (n=6) injected by tail vein. Xenograft tumors were quantified by luciferase - photon signals with Xenogen software. ** P< 0.001; * P< 0.01 compared to the control group. Error bars indicate S.E.M. The whole-mouse (right upper panel) or an ex vivo GI (right down panel) representative imaging is shown in (C).

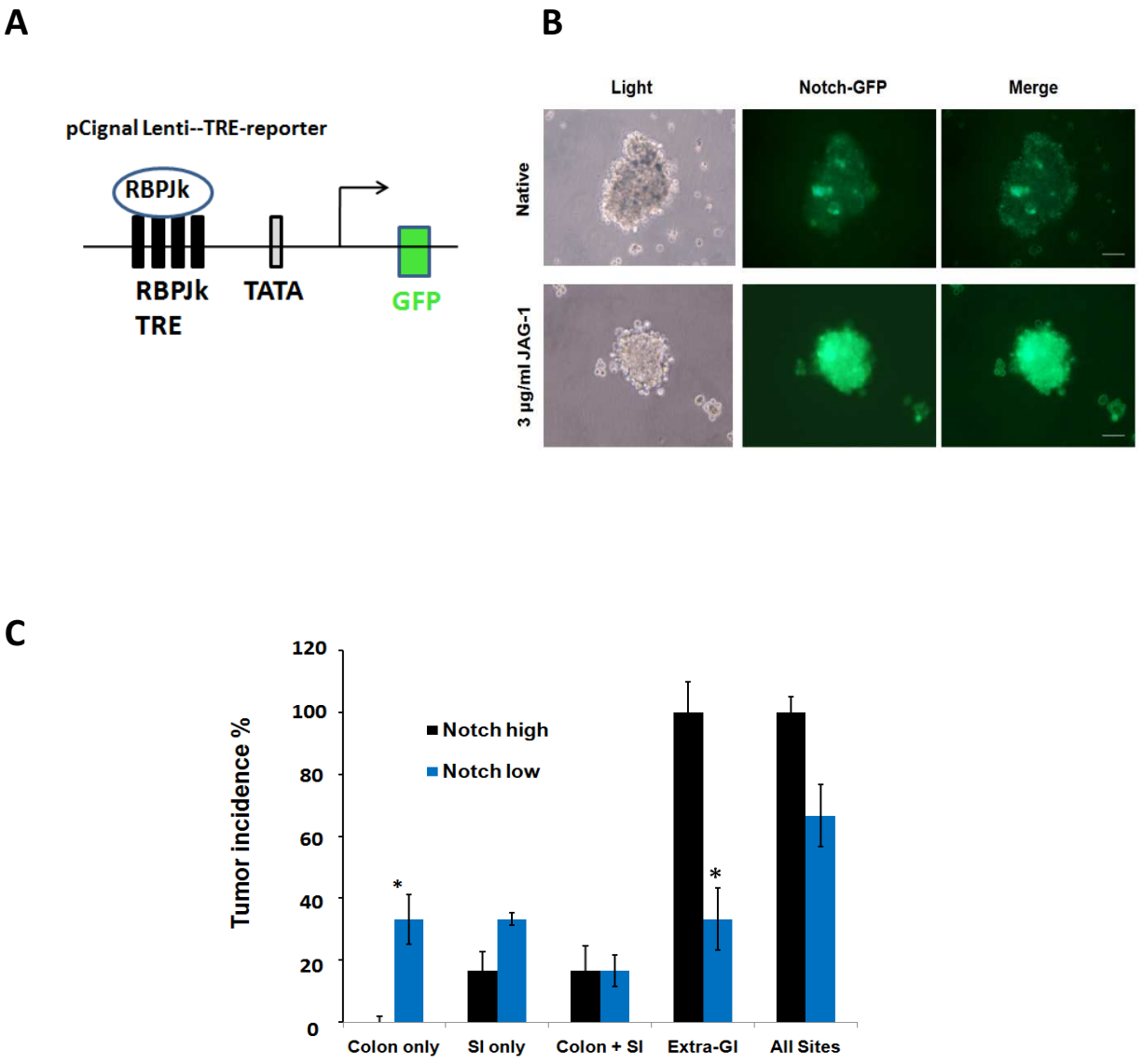

Supplemental Figure 7. related to Figure 8.CCICNotch reporter cells and *in vivo* xenografts formed by Notch high and Notch low CCICs. (A) schematic of Notch GFP reporter vector which has tandem repeats of RBP-Jk transcription responsive elements (TRE) binding to Notch downstream transcriptional factor RBP-Jk, activating promoter (TATA) and GFP expression. **(B)**CCIC Native Notch signaling was detected by GFP and increased when treated with 3µg/ml JAG1 for 4-6 hours. Scale bar, 20µ.**(C)**Xenograft tumor incidence in mice injected with FACS sorted GFP-Notch high or GFP-Notch low CCIC, organized by tumor site. * P< 0.01 compared to mock control. Error bars indicate S.E.M.

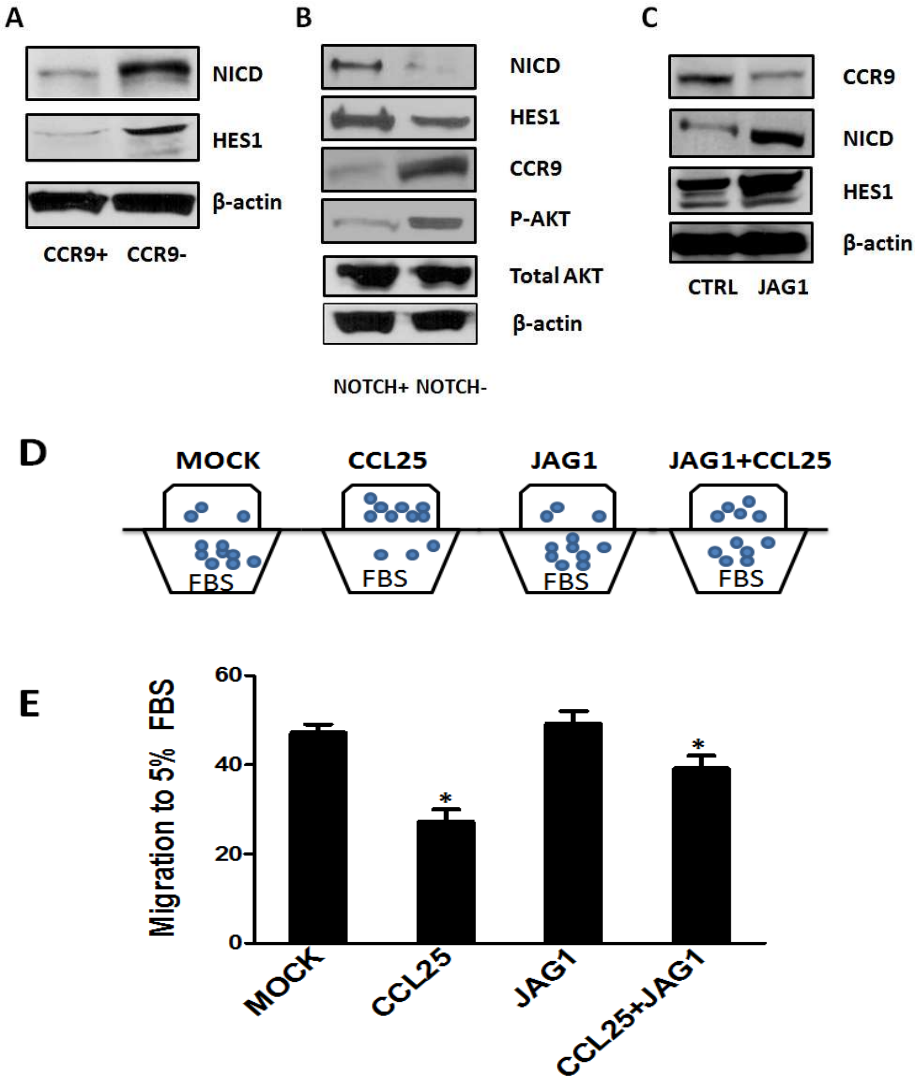

Supplemental Figure 8. Related to Figure 8. NOTCH downregulates CCR9/CCL25 axis signaling in early stage CCIC, and early stage CCIC chemotaxis to 5% FBS is inhibited by CCL25 and partially restored by *JAG1* (A)CCR9+ CCIC have lower NICD and *HES1* levels vs. CCR9- CCIC as shown by western blot. (**B).** GFP-NOTCH reporter CCIC were sorted into high and low NOTCH signaling sub-populations by FACS; CCR9 and phospho-AKT (ser 473) levels were detected higher in GFP-NOTCH- CCIC, but with no change in total AKT levels. NICD, HES1 and β-actin levels are shown for comparison. (**C)** Pre-treatment of CCR9+ CCIC with 2μg/ml *JAG1* peptide for 8 hours decreases CCR9 protein expression. NICD and HES1 levels are shown for comparison. (**D**) Schematic of CCIC incubated with different ligands in different chambers. Blue dots are representative of the relative number of cells in each chamber. FBS, 5% fetal bovine serum. (**E**) Graph of the percentage of early stage CCIC migrating to 5% FBS (%). The ligands match the schematic in (**D**). *P<0.001 by one way ANOVA for comparisons of mock control vs. CCL25 or *JAG1* vs. CCL25+*JAG1* data points.

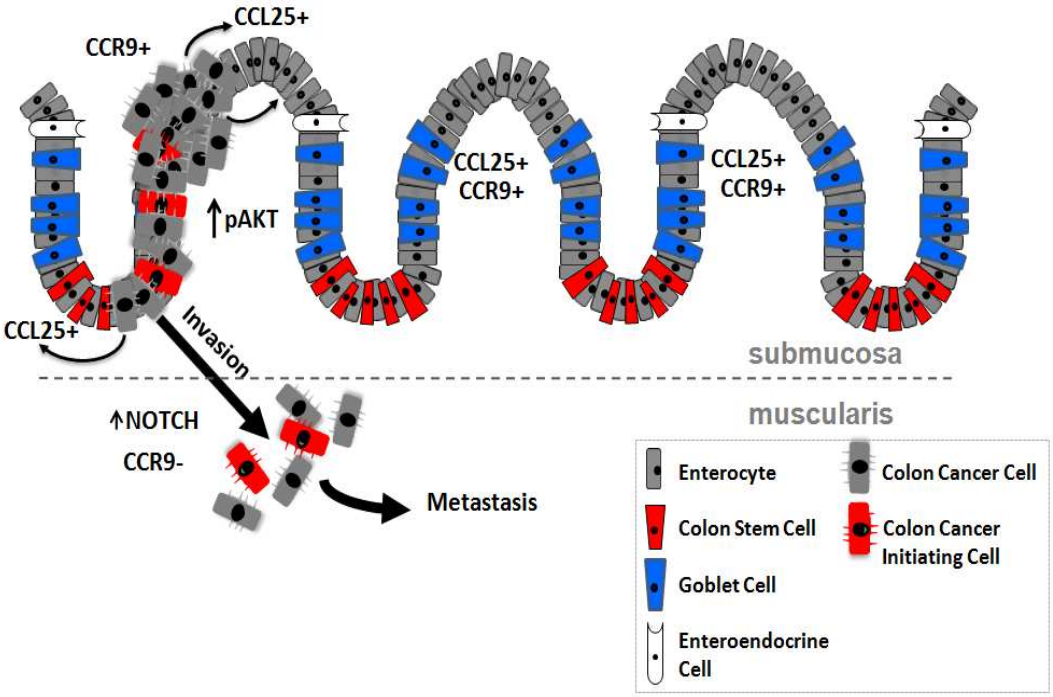

Supplemental Figure 9. Model figure of CCR9/CCL25 in the evolution of early stage to advanced CRC. Normal colon is schematized, with the crypt base on the bottom and crypt mouth at the top of the figure. A legend is given for each of the major normal colon cell types, as well as colon cancer cells and colon cancer stem cells. Early stage non-invasive CCIC and non-CCIC CRC cells upregulate the CCR9 receptor. Paracrine CCL25 from adjacent normal colon upregulates AKT signaling, proliferation, anti-apoptosis and likely superficial tumor spread along mucosal margins. As tumors progress, some cells upregulate NOTCH signaling (perhaps in response to NOTCH ligand expressing tumor associated cells such as vascular endothelium). Upregulation of NOTCH signaling causes an “invasive switch” that suppresses CCR9 and promotes NOTCH driven invasion and metastasis. Invasive and metastatic CRC tumors do not express CCR9, and CCL25 is absent from metastatic sites.

A

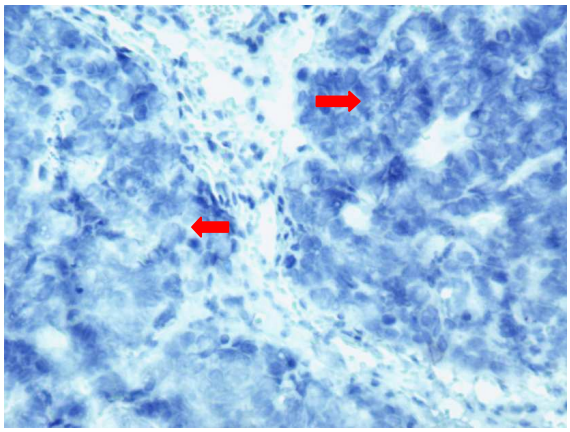

B

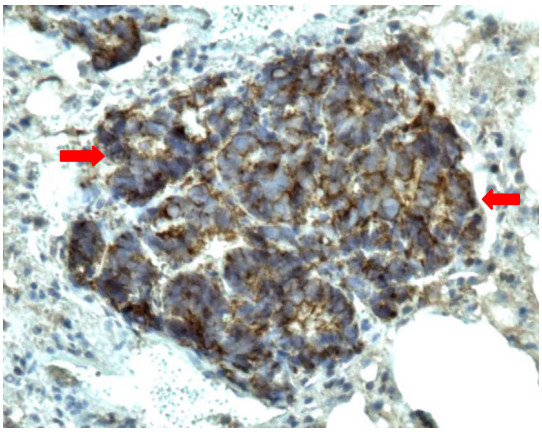

Supplemental Figure 10. CXCR4 expression in early stage CCIC extra-GI tumor. CXCR4 protein detected by immunohistochemistry in xenograft lung tumors, shown by DAB (brown), (A) IgG control; (B) anti-human CXCR4 antibody; red arrows designate tumor foci.

Supplemental Table 1: Primary human colorectal cancers used for CCR9 FACS, chemotaxis, p-AKT and cell proliferation analyses

ID	Age	Gender	Stage	Histopathology	Assays[a]
1	81	M	I	Adenocarcinoma, moderately differentiated	FACS/ p-AKT/ chemotaxis
2	74	M	I	Adenocarcinoma, moderately differentiated	FACS/ p-AKT/ chemotaxis
3	70	F	I	Adenocarcinoma, well to moderately differentiated	FACS/ p-AKT/ chemotaxis
4	86	F	II	Adenocarcinoma, well to moderately differentiated	FACS/ chemotaxis
5	58	M	II	Adenocarcinoma, well to moderately differentiated	FACS/ chemotaxis
6	63	M	I	Adenocarcinoma, well to moderately differentiated	FACS/ chemotaxis
7	59	F	II	Adenocarcinoma, poorly differentiated	FACS/ chemotaxis
8	90	F	II	Adenocarcinoma, poorly differentiated	FACS/ Proliferation
9	85	M	I	Adenocarcinoma, poorly differentiated	FACS/ Proliferation
10	40	M	II	Adenocarcinoma, poorly differentiated	FACS

[a] **The primary CRC cells were used for the assays of FACS, chemotaxis function, AKT phospholation or cell proliferation.**

Supplemental Table 2: Colorectal Cancer Initiating Cell Lines used for multiple analyses

ID	Age	Gender	Stage	Histopathology	Assays[a]
(early stage) CCIC1	57	M	I	Adenocarcinoma, well to moderately differentiated	FACS/ Mouse/ p-AKT/ Chemotaxis/ Proliferation / Western/ Q-PCR/ Microarray
(early stage) CCIC2	51	M	II	Adenocarcinoma, well differentiated	FACS/ Mouse/ p-AKT/ Chemotaxis/ Proliferation / Western/ Q-PCR
(early stage) CCIC3	74	F	I	Adenocarcinoma, well to moderately differentiated	FACS/ Mouse/ Western
(late stage) CCIC1	54	M	III	Adenocarcinoma, moderately differentiated	FACS/ Mouse/ Chemotaxis/ Western
(late stage) CCIC2	61	M	IV	Carcinoma, poor to moderately differentiated (liver metastasis)	FACS/ Mouse/ Western

[a] **The CCIC cells were used for the assays of FACS, in vivo mouse study, chemotaxis function, AKT phospholation, cell proliferation, western blot, quantative PCR, or micro-array.**